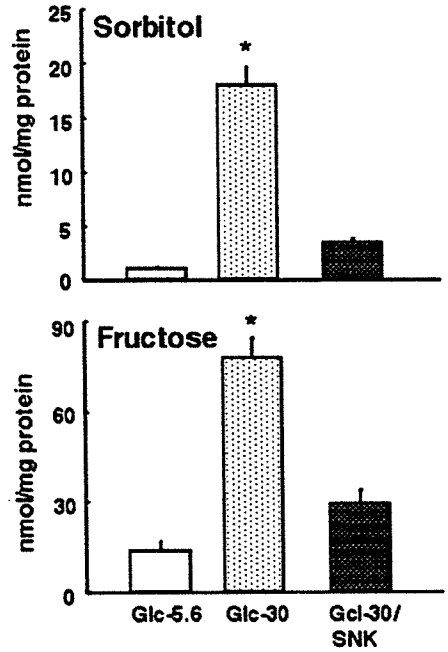

Fig. 5 Intracellular contents of sorbitol (upper panel) and fructose (lower panel) determined by liquid-chromatography. Values expressed as nmol/mg protein represent the mean + SEM of four experiments. *$p < 0.01$ as compared with Glc-5.6 or Glc-30/SNK.

from primary and long-term cultured Schwann cells in that the former were not contact inhibited and formed ball-shaped subcolonies when cultures reached confluence (Watabe *et al.* 1995). We failed to show that the cell line could myelinate a mouse axon (Watabe *et al.* unpublished observations), in the same way as endogenous Schwann cells in the peripheral nerves and primary cultured Schwann cells (Suzuki *et al.* 1999). In spite of those differences from normal Schwann cells, IMS32 cells have advantages for the study of diabetic neuropathy, such as the activation of the polyol pathway (shown in this study) and the decreased proliferative activity (Kato *et al.* 2003; Nakamura *et al.* 2003) under high glucose conditions mimicking hyperglycaemia *in vivo*.

Activation of the polyol pathway in IMS32 under high glucose (≥ 30 mM) environments

In the present study, we observed the significant up-regulation of the mRNA expression for AR and SDH and protein expression for AR under Glc-56 (Figs 2 and 3), and marked increases in the intracellular sorbitol and fructose contents under Glc-30 (Fig. 5) and Glc-56 (beyond the range of measurement), compared with those under Glc-5.6. Although not statistically significant, AR expressions at both mRNA and protein levels under Glc-30 were approximately 1.8-fold higher than those under Glc-5.6. These findings were in line with the enhanced AR immunoreactivity under Glc-30 according to immunocytochemistry (Fig. 4). We did not measure the enzyme activity in the cells, but the excessive production of sorbitol and fructose under Glc-30 and Glc-56 suggests the high glucose-induced activation of AR and SDH. Furthermore, the application of an AR inhibitor, SNK-860, to Glc-30 for 7 days diminished the intracellular polyol contents to a level close to Glc-5.6. Taking these findings together, the exposure of IMS32 to the high glucose (≥ 30 mM) environments is likely to enhance the expression and activity of AR, thereby leading to exaggerated flux through the polyol pathway. Significant up-regulation of mRNA and protein expressions for AR under Glc-56 and NaCl-50 suggests that AR is induced by not only high glucose but hyperosmotic conditions. The increased expression of AR under hyperosmotic environments has been reported in a variety of cells, and indicates the osmoregulatory role of AR (Yabe-Nishimura 1998). Compared with AR, much less information is available concerning the expression of SDH. The mRNA expression of SDH was not induced by hyperosmolality in rat Schwann cells (Maekawa *et al.* 2001) or renal collecting duct cells (Grunewald *et al.* 1998). Those findings are contrary to the results in this study, i.e. the significant up-regulation of SDH mRNA expression under Glc-56 and NaCl-50. Although the reasons for such variable results among the cells are unknown, we clearly demonstrated that the exposure to high glucose or hyperosmotic environments could induce both AR and SDH mRNA in IMS32.

It remains to be elucidated why an increase in the glucose concentration to 20–30 mM, corresponding to the plasma level in poorly controlled diabetic patients, accelerated the polyol pathway in IMS32, but not in other cultured Schwann cells (Mizisin *et al.* 1996; Suzuki *et al.* 1999; Maekawa *et al.* 2001). In adult rat Schwann cells, neither AR expression/activity nor intracellular sorbitol levels were enhanced under 30-mM glucose conditions. However, the extracellular sorbitol level under those conditions was increased significantly compared with that in the 5.6-mM glucose conditions (Suzuki *et al.* 1999). These findings suggested that sorbitol was released from the cells into the media by an unidentified transport mechanism. In JS1 Schwannoma cells, sorbitol did not accumulate under 25 mM glucose nor 100 mM NaCl conditions unless a SDH inhibitor was applied (Mizisin *et al.* 1997). In contrast with those cells, conspicuous increases of intracellular sorbitol (18-fold) and fructose (6-fold) levels were observed in IMS32 under Glc-30. It seems possible that IMS32 cells possess a much higher capacity than other Schwann cells to store sorbitol and other glucose-derived metabolites. To verify this possibility, we are now investigating if the levels of dicarbonyl intermediates, such as methylglyoxal and 3-deoxyglucosone (Kikuchi *et al.* 1999) in IMS32, are elevated under Glc-30. It is also noteworthy that immortalized Schwann cells were established from not only normal

Table 1 Alteredgene expressino in IMS32 under the high glucose ([Glc-30]) versus normal glucose ([Glc-5.6]) condition

GenBank Accession No.	Gene	Molecular Function	Ratio ([Glc-30]/[Glc-5.6])
Up-regulated			
AK003182	Myosin light chain, alkali, fast skel.	calcium ion binding (cytoskeleton organization and biogenesis)	2.04
NM_008182	Glutathione S-transferase alpha 2	glutathione transferase activity (detoxification of lipid aldehydes)	2.46
NM_009426	Thyrotropin-releasing hormone (TRH)	thyrotropin-releasing hormone activity	2.04
NM_011315	Serum amyloid A3 (SAA3)	acute-phase response protein activity, lipid transporter activity	2.61
NM_020581	Angiopoietin-like 4 (ANGPTL4)	inhibiting lipoprotein lipase activity, angiogenesis	2.3
NM_023557	RIKEN cDNA 2210409D01	unknown	3.35
NM_144731	UDP-N-acetyl-alpha-D-galactosamine:polypeptide N-acetyl-galactosaminyl transferase (GALNT7)	polypeptide N-acetylgalactosaminyltransferase activity, transferase activity, transferring glycosyl groups	2.43
NM_144876	RIKEN cDNA D930050H05	unknown	3.21
NM_145492	Ecotropic viral integration site3 (Evi-3)	a retroviral integration site in murine B-cell lymphoma	3.13
NM_146720	Olfactory receptor 421 (Olfr421)	olfactory receptor function	2.05
Down-regulated			
AK019076	Adult male tongue cDNA (RAP1 GTPase activating protein 1H)	unknown	0.37
NM_008474	Type II 65kd keratin (KRT-2-16)	structural constituent of cytoskeleton	0.44
NM_007392	Alpha 2 actin	structural constituent of cytoskeleton	0.49
NM_007810	Cytochrome P450, 19, aromatase (Cyp19)	monooxygenase activity, oxidoreductase activity	0.45
NM_008522	Lactotransferrin	ferric iron binding	0.43
NM_008826	Phosphofructokinase	6-phosphofructokinase activity (glycolysis)	0.49
NM_009075	Ribose 5-phosphate isomerase	ribose-5-phosphate isomerase activity (pentose-phosphate shunt)	0.44
NM_010266	Guanine deaminase	hydrolase activity	0.43
NM_011144	Peroxisome proliferation activated receptor alpha (PPARα)	transcription factor activity (regulation of fatty acid metabolism)	0.45
NM_013549	Histone2, H2AA1	unknown	0.34
NM_013713	Keratin associated protein 15	unknown (differentiation of epithelial cells?)	0.29
NM_018873	P140 protein	controlling actin cytoskeleton organization	0.42
NM_019467	Allograft inflammation factor 1 (AIF1)	a potential modulator of macrophage activation	0.43
NM_019752	Serine protease (Prss25)	serine-type endopeptidase activity (proteolysis, apoptosis)	0.37
NM_020009	FK506 binding protein associated protein 1 (FRAP1)	inositol/phosphatidylinositol kinase activity	0.27
NM_021473	Aldo-keto reductase (AKR1A4)	aldehyde reductase activity , oxidoreductase activity	0.39
NM_023115	Protocadherin 15 (PCDH15)	calcium ion binding (homophilic cell adhesion)	0.19
NM_024464	RIKEN cDNA 2010319C14	unknown	0.24
NM_025692	RIKEN cDNA 5730525G14	unknown	0.28

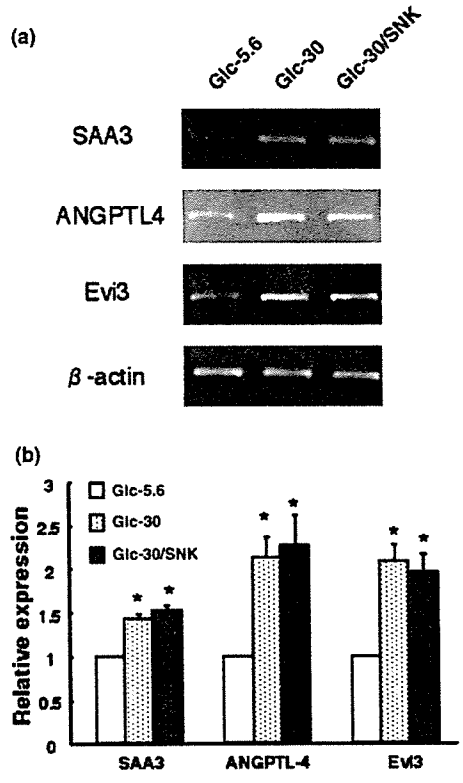

Fig. 6 Relative mRNA expressions of serum amyloid A3 (SAA3), angiopoietin-like 4 (ANGPTL4) and ecotropic viral integration site 3 (Evi3) in IMS32 determined by semiquantitative RT–PCR. (a) Gel electrophoresis show more intense signals for SAA3, ANGPTL4 and Evi3 mRNA in Glc-30 and Glc-30/SNK than in Glc-5.6. (b) The mRNA expressions of SAA3, ANGPTL4 and Evi3 in Glc-30 and Glc-30/SNK relative to those in Glc-5.6. Values represent the mean + SEM of four experiments. $^*p < 0.05$ as compared with Glc-5.6.

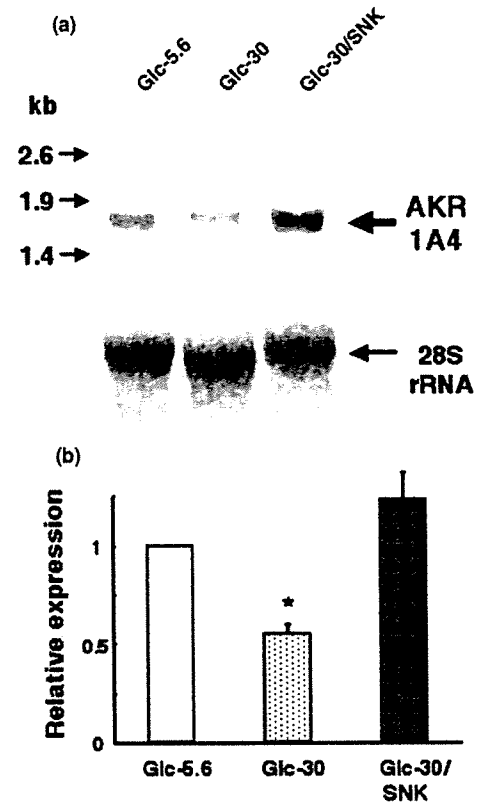

Fig. 7 Relative mRNA expression of aldehyde reductase (AKR1A4) in IMS32 determined by northern blot analysis. (a) The picture of the blot hybridized with an alkaline–phosphatase-labelled cDNA probe (upper panel). mRNA for AKR1A4 was detected as a single band corresponding to a molecular weight of around 1.7 kb. The blot showed a less intense signal for AKR1A4 mRNA in Glc-30 than that in Glc-5.6 or Glc-30/SNK. A methylene blue-stained image (28S ribosomal RNA) of the duplicate membrane (lower panel) showed that a relatively equal amount of RNA was loaded. (b) The mRNA expression of AKR1A4 in Glc-30 and Glc-30/SNK relative to that in Glc-5.6. Values represent the mean + SEM of four experiments. $^*p < 0.05$ as compared with Glc-5.6 or Glc-30/SNK.

adult mice but also from mouse models of metabolic diseases such as Niemann–Pick disease type C (NPC; *spm/spm*, npc^{nih}/npc^{nih}; Watabe *et al.* 2001, 2003), globoid cell leukodystrophy (twitcher; Shen *et al.* 2002) and G_{M2} gangliosidosis (Ohsawa *et al.* 2005). The cells originated from those mouse models were able to survive and proliferate in culture, despite the progressive accumulation of undegraded substrates in the cytoplasm.

High glucose-induced alterations of gene expression profiles in IMS32

In recent studies, gene expression pattems in DRG (Burnand *et al.* 2004), superior mesenteric and celiac ganglia (SMG-CG) and superior cervical ganglia (SCG) (Carroll *et al.* 2004) were compared between streptozotocin (STZ)-diabetic and control rats via microarray profiling. Those approaches appear to be useful to elucidate the molecular mechanism of the development of diabetic neuropathy. However, the peripheral ganglia contain neurons, Schwann cells and other cells, and the microarray studies on them are not sufficient to specify the cells with altered gene expressions. By employing DNA microarray and subsequent RT–PCR or northern blot analyses, we investigated the gene expression profiles in IMS32 exposed to normal (Glc-5.6) and high (Glc-30) glucose conditions. Because 30 mM glucose in culture medium (Glc-30) is closer to the blood glucose concentration in diabetic individuals than 56 mM (Glc-56), we thought that the findings from the comparison between Glc-30 and Glc-5.6 could be more relevant to the *in vivo* studies between diabetic and normal conditions. Although the expression of AR mRNA/protein was not significantly up-regulated by exposure to Glc-30 (Figs 2 and 3, and Table 1), intracellular contents of sorbitol and fructose under

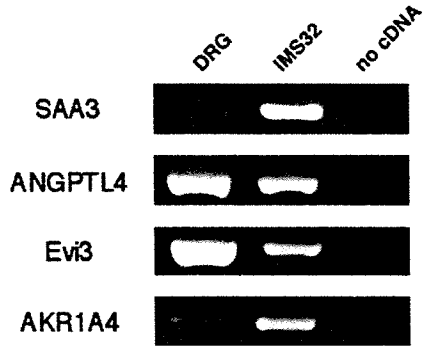

Fig. 8 mRNA expression of SAA3, ANGPTL4, Evi3 and AKR1A4 in the peripheral nerves of an adult mouse: RT–PCR analysis. The pictures of gel electrophoresis showed the PCR products from the cDNA of adult mouse DRG associated with spinal nerve bundles, IMS32 cells, and PCR reactions without a template cDNA, respectively.

Glc-30 were markedly higher than those under Glc-5.6. It seems possible that the degree of increases in the enzyme activity of AR does not correlate with that in the mRNA/protein expression in IMS32 under Glc-30.

The microarray analysis revealed 10 up-regulated genes and 18 down-regulated genes under the high glucose conditions (Table 1). Among the up-regulated molecules, glutathione S-transferase α2 (GSTα2) is an isozyme of GST and may be involved in the detoxification of lipid peroxidation products generated by oxidative stress under hyperglycaemic conditions (Srivastava *et al.* 1995; Obrosova 2002). Among the down-regulated genes, phosphofructokinase, one of the key glycolytic enzymes, is essential for the maintenance of axonal integrity; endogenous aldehydes originating from the lipid-peroxidation process are potent inhibitors of this enzyme and may cause significant nerve damage (Novotny *et al.* 1994). Peroxisome proliferator-activated receptor α (PPARα) is an isotype of PPAR, transcription factors involved in the regulation of. lipid and glucose metabolism (Staels and Fruchart 2005). Shibata *et al.* (2000) observed that treatment with JTT501, a PPARα and -γ agonist, prevented the development of diabetic neuropathy in Zucker diabetic fatty rats. However, further RT–PCR/northern blot analyses failed to show the high glucose-induced changes of expression of these genes. In contrast, these analyses confirmed the microarray results, such as significant up-regulation of mRNA expressions for SAA3, ANGPTL4 and Evi3, and the down-regulation of aldehyde reductase (AKR1A4) mRNA expression.

SAA3

Serum amyloid A (SAA), a family of apolipoproteins associated with high-density lipoprotein, is known as an acute-phase reactant (Meek *et al.* 1992). There is an increasing body of evidence that correlates the diabetic conditions with the chronic elevation of SAA (Hamano *et al.* 2004) and the up-regulation of SAA3 (Lin *et al.* 2001), but their significance remains to be elucidated. SAA, as well as advanced glycation end products (AGE), is one of the ligands for the receptor for AGE (RAGE) and the RAGE–ligand interaction is likely to induce cellular dysfunction, thereby being implicated in the development of diabetic complications (Schmidt *et al.* 2000). In addition, Chung *et al.* (2000) observed intense immunoreactivity for SAA in the brains of patients with neurodegenerative diseases such as Alzheimer's disease and multiple sclerosis; the major site of SAA staining in both diseases was the myelin sheaths and axonal membrane. Taking this finding, together with the evidence that SAA can inhibit lipid biosynthesis (Schreiber *et al.* 1999), up-regulation of SAA in nervous tissue under hyperglycaemic conditions might affect myelin lipid synthesis.

ANGPTL4

The ANGPTL4 gene is predominantly expressed in the adipose tissue and liver, but its induction in ischaemic tissues (Le Jan *et al.* 2003) implies a role of this molecule in the compensatory angiogenesis for ischaemia and hypoxia (Deindl *et al.* 2001). ANGPTL4 is recognized as a downstream target gene of PPARα and -γ (Kersten *et al.* 2000), and induces hyperlipidaemia by inhibiting lipoprotein lipase (LPL) activity (Yoshida *et al.* 2002). LPL is expressed in cultured Schwann cells and may play a role in myelin phospholipid biosynthesis in the peripheral nervous system (Huey *et al.* 1998). Ferreira *et al.* (2002) reported that the activity of LPL in the sciatic nerves was reduced in STZ-diabetic rats and restored by treatment with insulin. Taking these findings into consideration, it seems possible that up-regulated ANGPTL4 in Schwann cells under hyperglycaemic conditions inhibits LPL activity, thereby being one of the causes for the impaired fatty acid metabolism and deficient phospholipid synthesis in nervous tissue (Cameron *et al.* 1998; Martin *et al.* 2003). SAA may also play a role in the lipid synthesis as described above, but the interaction between the two molecules remains unknown.

Evi3

Evi3 is a common retroviral integration site in murine B-cell lymphoma and encodes a novel zinc finger protein (Warming *et al.* 2003). Because very few papers described this molecule (most of them were focused on tumorigenesis in haematopoietic cells), we currently have no information or idea of how this molecule is involved in the pathobiology of diabetic neuropathy. Treatment with SNK-860 had no effects on the mRNA expressions for SAA3, ANGPTL4 or Evi3 under Glc-30 in this study. This finding suggests that the

up-regulation of these genes in IMS32 under high glucose conditions is not related to the polyol pathway hyperactivity.

AKR1A4

Aldehyde reductase is a member of the aldo–keto reductase (AKR) superfamily (the AKR1A subfamily represents the aldehyde reductases and the AKR1B subfamily represents the aldose reductases) (Allan and Lohnes 2000; Hyndman *et al.* 2003). Approximately 50% of the amino acid sequences are conserved between aldehyde reductase and AR (Bohren *et al.* 1989), and both enzymes catalyze the reduction of reactive biogenic aldehydes [e.g. glyceraldehyde, methylglyoxal (MG), hydroxynonenal (HNE) and glucosones] by using NADPH as a cofactor (Flynn 1986; Vander Jagt *et al.* 1992). Unlike AR, aldehyde reductase is virtually inactive for glucose and other aldo sugars (Kawasaki *et al.* 1989). Consequently, much less attention has been paid to aldehyde reductase than AR in the research field of diabetes and its complications (Takahashi *et al.* 1995; Danesh *et al.* 2003). In the present study, reduced mRNA expression of aldehyde reductase in IMS32 under high glucose conditions was completely ameliorated by treatment with an AR inhibitor, SNK-860. The activated AR enhances the flux through the polyol pathway by converting glucose to sorbitol, but it may also act against reactive aldehydes and related substances produced by lipid peroxidation and oxidative stress under hyperglycaemic conditions (Rittner *et al.* 1999; Obrosova 2002). Like AR, aldehyde reductase appears to be able to neutralize lipid peroxidation products (Suzuki *et al.* 1998), but the results in this study suggest that the production of this enzyme is suppressed by augmented expression and activity of AR in Schwann cells during hyperglycaemic conditions. Conversely, AR inhibition may up-regulate aldehyde reductase to be more active against the toxic substances induced by high glucose. This idea is partly supported by findings from previous studies which suggested the functional redundancy of the two enzymes in rat sympathetic ganglia (Kawamura *et al.* 1999, 2002). Moreover, a lack of apparent phenotypes, except a slightly defective urine-concentrating ability in AR-knockout mice (Ho *et al.* 2000), led us to speculate that the detoxification function may be taken over by aldehyde reductase in the absence of AR. However, there has been no direct evidence to indicate such redundancy of these enzymes under hyperglycaemic conditions. It is also important to note that aldehyde dehydrogenase (ALDH) and alcohol dehydrogenase (ADH), as well as AR and aldehyde reductase, can participate in the detoxification of reactive aldehydes in nervous tissue (Picklo *et al.* 2001). A recent report by Suzuki *et al.* (2004) implied the association of the ALDH2/ADH2 polymorphism with the development of human diabetic neuropathy. We expect that further studies focusing on the expression and activity of aldehyde reductase in the peripheral nervous system under hyperglycaemic conditions, especially in relation to those of AR, ALDH and ADH, will elucidate the role of this enzyme in the pathogenesis of diabetic neuropathy.

The mRNA expression of SAA3, ANGPTL4, Evi3 and AKR1A4 in DRG and spinal nerves in adult normal ICR mice (Fig. 8) suggests their functional roles in the peripheral nervous system. We are about to determine if the expression of these genes is altered in the nerves of STZ-diabetic mice. The antibodies to these proteins are not available from a commercial source, and we plan to collaborate with laboratories studying these molecules. Future studies with the antibodies will help elucidate the immunochemical localization and function of these proteins in the peripheral nervous system and their involvement in the pathogenesis of diabetic neuropathy.

Conclusion

The findings in this study indicate the activation of the polyol pathway and the altered gene expression profiles (i.e. up-regulation of SAA3, ANGPTL4 and Evi3 mRNA and down-regulation of AKR1A4 mRNA) in IMS32 under exposure to a high glucose (≥ 30 mM) environment. Considering that an increase in glucose concentration to 20–30 mM accelerated the polyol pathway in IMS32, but not in other previously reported Schwann cells, the culture system of IMS32 under high glucose conditions may provide useful information about the pathogenesis of diabetic neuropathy, especially polyol pathway-related abnormalities.

Acknowledgements

This work was supported by a Grant-in-aid for Scientific Research from the Japanese Ministry of Education, Science, Sports and Culture, and grants from the Sanwa Kagaku Kenkyusho, Suzuken Memorial Foundation and the Japan Diabetes Foundation. We thank Drs Hitoshi Kawano, Koichi Kato, Noriaki Kato and Miwa Sango-Hirade for the helpful suggestions, and Akiko Tokashiki and Kyoko Ajiki for their technical assistance.

References

Allan D. and Lohnes D. (2000) Cloning and developmental expression of mouse aldehyde reductase (AKR1A4). *Mech. Dev.* **94**, 271–275.

Bohren K. M., Bullock B., Wermuth B. and Gabbay K. H. (1989) The aldo-keto reductase superfamily. cDNAs and deduced amino acid sequences of human aldehyde and aldose reductases. *J. Biol. Chem.* **264**, 9547–9551.

Burnand R. C., Price S. A., McElhaney M., Barker D. and Tomlinson D. R. (2004) Expression of axotomy-inducible and apoptosis-related genes in sensory nerves of rats with experimental diabetes. *Brain Res. Mol. Brain Res.* **132**, 235–240.

Cameron N. E., Cotter M. A., Horrobin D. H. and Tritschler H. J. (1998) Effects of α-lipoic acid on neurovascular function in diabetic rats: interaction with essential fatty acids. *Diabetologia* **41**, 390–399.

Carroll S. L., Byer S. J., Dorsey D. A., Watson M. A. and Schmidt R. E. (2004) Ganglion-specific patterns of diabetes-modulated gene

expression are established in prevertebral and paravertebral sympathetic ganglia prior to the development of neuroaxonal dystrophy. *J. Neuropathol. Exp. Neurol.* **63**, 1144–1154.

Chung T. F., Sipe J. D., McKee A., Fine R. E., Schreiber B. M., Liang J. S. and Johnson R. J. (2000) Serum amyloid A in Alzheimer's disease brain is predominantly localized to myelin sheaths and axonal membrane. *Amyloid* **7**, 105–110.

Danesh F. R., Wada J., Wallner E. I., Sahai A., Srivastava S. K. and Kanwar Y. S. (2003) Gene regulation of aldose-, aldehyde- and a renal specific oxido reductase (RSOR) in the pathobiology of diabetes mellitus. *Curr. Med. Chem.* **10**, 1399–1406.

Deindl E., Buschmann I., Hoefer I. E., Podzuweit T., Boengler K., Vogel S., van Royen N., Fernandez B. and Schaper W. (2001) Role of ischemia and of hypoxia-inducible genes in arteriogenesis after femoral artery occlusion in the rabbit. *Circ. Res.* **89**, 779–786.

Dyck P. J. and Giannini C. (1996) Pathologic alterations in the diabetic neuropathies of humans: a review. *J. Neuropathol. Exp. Neurol.* **55**, 1181–1193.

Eckersley L. (2002) Role of the Schwann cell in diabetic neuropathy. *Int. Rev. Neurobiol.* **50**, 293–321.

Ferreira L. D., Huey P. U., Pulford B. E., Ishii D. N. and Eckel R. H. (2002) Sciatic nerve lipoprotein lipase is reduced in streptozotocin-induced diabetes and corrected by insulin. *Endocrinology* **143**, 1213–1217.

Flynn T. G. (1986) Aldose and aldehyde reductase in animal tissues. *Metabolism* **35**, 105–108.

Grunewald R. W., Wagner M., Schubert I., Franz H. E., Muller G. A. and Steffgen J. (1998) Rat renal expression of mRNA coding for aldose reductase and sorbitol dehydrogenase and its osmotic regulation in inner medullary collecting duct cells. *Cell Physiol. Biochem.* **8**, 293–303.

Guerrant G. and Moss C. W. (1984) Determination of monosaccharides as aldononitrile, *O*-methyoxime, alditol, and cyclitol acetate derivatives by gas chromatography. *Anal. Chem.* **56**, 633–638.

Gui T., Tanimoto T., Kokai Y. and Nishimura C. (1995) Presence of a closely related subgroup in the aldo–keto reductase family of the mouse. *Eur. J. Biochem.* **227**, 448–453.

Hamano M., Saito M., Eto M., Nishimatsu S., Suda H., Matsuda M., Matsuki M., Yamamoto S. and Kaku K. (2004) Serum amyloid A, C-reactive protein and remnant-like lipoprotein particle cholesterol in type 2 diabetic patients with coronary heart disease. *Ann. Clin. Biochem.* **41**, 125–129.

Ho H. T., Chung S. K., Law J. W., Ko B. C., Tam S. C., Brooks H. L., Knepper M. A. and Chung S. S. (2000) Aldose reductase-deficient mice develop nephrogenic diabetes insipidus. *Mol. Cell Biol.* **20**, 5840–5846.

Huey P. U., Marcell T., Owens G. C., Etienne J. and Eckel R. H. (1998) Lipoprotein lipase is expressed in cultured Schwann cells and functions in lipid synthesis and utilization. *J. Lipid Res.* **39**, 2135–2142.

Hyndman D., Bauman D. R., Heredia V. V. and Penning T. M. (2003) The aldo–keto reductase superfamily homepage. *Chem. Biol. Interact.* **143–144**, 621–631.

Kato K., Nakamura J., Kamiya H. *et al.* (2003) Effect of high glucose and C-peptide on proliferation and MAP kinase activity in cultured immortalized mouse Schwann (IMS32) cells. *J. Peripher. Nerv. Syst. (Abstr.)* **8**, 183.

Kawamura M., Eisenhofer G., Kopin I. J. *et al.* (1999) Aldose reductase, a key enzyme in the oxidative deamination of norepinephrine in rats. *Biochem. Pharmacol.* **58**, 517–524.

Kawamura M., Eisenhofer G., Kopin I. J., Kador P. F., Lee Y. S., Fujisawa S. and Sato S. (2002) Aldose reductase: an aldehyde scavenging enzyme in the intraneuronal metabolism of norepinephrine in human sympathetic ganglia. *Auton. Neurosci.* **96**, 131–139.

Kawasaki N., Tanimoto T. and Tanaka A. (1989) Characterization of aldose reductase and aldehyde reductase from rat testis. *Biochim. Biophys. Acta* **996**, 30–36.

Kern T. S. and Engerman R. L. (1982) Immunohistochemical distribution of aldose reductase. *Histochem. J.* **14**, 507–515.

Kersten S., Mandard S., Tan N. S., Escher P., Metzger D., Chambon P., Gonzalez F. J., Desvergne B. and Wahli W. (2000) Characterization of the fasting-induced adipose factor FIAF, a novel peroxisome proliferator-activated receptor target gene. *J. Biol. Chem.* **275**, 28 488–28 493.

Kikuchi S., Shinpo K., Moriwaka F., Makita Z., Miyata T. and Tashiro K. (1999) Neurotoxicity of methylglyoxal and 3-deoxyglucosone on cultured cortical neurons: synergism between glycation and oxidative stress, possibly involved in neurodegenerative diseases. *J. Neurosci. Res.* **57**, 280–289.

Le Jan S., Amy C., Cazes A. *et al.* (2003) Angiopoietin-like 4 is a proangiogenic factor produced during ischemia and in conventional renal cell carcinoma. *Am. J. Pathol.* **162**, 1521–1528.

Lee F. K., Lee A. Y. W., Lin C. X. F. *et al.* (1995) Cloning, sequencing, and determination of the sites of expression of mouse sorbitol dehydrogenase cDNA. *Eur. J. Biochem.* **230**, 1059–1065.

Lin Y., Rajala M. W., Berger J. P., Moller D. E., Barzilai N. and Scherer P. E. (2001) Hyperglycemia-induced production of acute phase reactants in adipose tissue. *J. Biol. Chem.* **276**, 42 077–42 083.

Low P. A., Nickander K. K. and Scionti L. (1999) Role of hypoxia, oxidative stress, and excitatory neurotoxins in diabetic polyneuropathy, in *Diabetic Neuropathy* (Dyck, P. J. and Thomas, P. K., eds), pp. 317–329. W. B. Saunders, Philadelphia.

Maekawa K., Tanimoto T., Okada S., Suzuki T., Suzuki T. and Yabe-Nishimura C. (2001) Expression of aldose reductase and sorbitol dehydrogenase genes in Schwann cells isolated from rat: effects of high glucose and osmotic stress. *Brain Res. Mol. Brain Res.* **87**, 251–256.

Martin A., Komada M. R. and Sane D. C. (2003) Abnormal angiogenesis in diabetes mellitus. *Med. Res. Rev.* **23**, 117–145.

Meek R. L., Eriksen N. and Benditt E. P. (1992) Murine serum amyloid A3 is a high-density apolipoprotein and is secreted by macrophages. *Proc. Natl Acad. Sci. USA* **89**, 7949–7952.

Mizisin A. P. and Powell H. C. (2003) Pathogenesis and pathology of diabetic neuropathy, in *Textbook of Diabetic Neuropathy* (Gries, F. A., Cameron, N. E., Low, P. A. and Ziegler, D., eds), pp. 83–169, Georg Thieme Verlag, New York.

Mizisin A. P., Li L., Perello M., Freshwater J. D., Kalichman M. W., Roux L. and Calcutt N. A. (1996) Polyol pathway and osmoregulation in JS1 Schwann cells grown in hyperglycemic and hyperosmotic conditions. *Am. J. Physiol.* **270**, F90–F97.

Mizisin A. P., Li L. and Calcutt N. A. (1997) Sorbitol accumulation and transmembrane efflux in osmotically stressed JS1 schwannoma cells. *Neurosci. Lett.* **229**, 53–56.

Nakamura J., Kamiya H., Nakae M., Naruse K., Hamada Y., Kato K. and Hotta N. (2003) Effect of bFGF on Schwann cell growth and diabetic neuropathy in rats. *J. Peripher. Nerv. Syst. (Abstr.)* **8**, 188–189.

Novotny M. V., Yancey M. F., Stuart R., Wiesler D. and Peterson R. G. (1994) Inhibition of glycolytic enzymes by endogenous aldehydes: a possible relation to diabetic neuropathies. *Biochem. Biophys. Acta.* **1226**, 145–150.

Obrosova I. G. (2002) How does glucose generate oxidative stress in peripheral nerve? *Int. Rev. Neurobiol.* **50**, 3–35.

Ohsawa M., Kotani M., Tajima Y. *et al.* (2005) Establishment of immortalized Schwann cells from a Sandhoff mouse and corrective effect of recombinant human β–hexosaminidase A on the accumulated GM2 ganglioside. *J. Hum. Genet.* **50**, 460–467.

Picklo M. J., Olson S. J., Markesbery W. R. and Montine T. J. (2001) Expression and activities of aldo–keto oxidoreductases in Alzheimer's disease. *J. Neuropathol. Exp. Neurol.* **60**, 686–695.

Pop-Busui R., Sullivan K. A., Van Huysen C., Bayer L., Cao X., Towns R. and Stevens M. J. (2001) Depletion of taurine in experimental diabetic neuropathy: implications for nerve metabolic, vascular, and functional deficits. *Exp. Neurol.* **168**, 259–272.

Rittner H. L., Hafner V., Klimiuk P. A., Szweda L. I., Goronzy J. J. and Weyand C. M. (1999) Aldose reductase functions as a detoxification system for lipid peroxidation products in vasculitis. *J. Clin. Invest.* **103**, 1007–1013.

Sango K., Horie H., Saito H., Ajiki K., Tokashiki A., Takeshita K., Ishigatsubo Y., Kawano H. and Ishikawa Y. (2002) Diabetes is not a potent inducer of neuronal cell death in mouse sensory ganglia, but it enhances neurite regeneration *in vitro*. *Life Sci.* **71**, 2351–2368.

Sango K., Tokashiki A., Ajiki K., Horie M., Kawano H., Watabe K., Horie H. and Kadoya T. (2004) Synthesis, localization and externalization of galectin-1 in mature dorsal root ganglion neurons and Schwann cells. *Eur. J. Neurosci.* **19**, 55–64.

Schmidt A. M., Yan S. D., Yan S. F. and Stern D. M. (2000) The biology of the receptor for advanced glycation end products and its ligands. *Biochim. Biophys. Acta* **1498**, 99–111.

Schreiber B. M., Veverbrants M., Fine R. E., Blusztain J. K., Salmona M., Patel A. and Sipe J. D. (1999) Apolipoprotein serum amyloid A down-regulates smooth-muscle cell lipid biosynthesis. *Biochem. J.* **344**, 7–13.

Shen J. S., Watabe K., Meng X. L., Ida H., Ohashi T. and Eto Y. (2002) Establishment and characterization of spontaneously immortalized Schwann cells from murine model of globoid cell leukodystrophy (twitcher). *J. Neurosci. Res.* **68**, 588–594.

Shibata T., Takeuchi S., Yokota S., Kamimoto K., Yonemori F. and Wakitani K. (2000) Effects of peroxisome proliferator-activated receptor-α and -γ agonist, JTT-501, on diabetic complications in Zucker diabetic fatty rats. *Br. J. Pharmacol.* **130**, 495–504.

Song Z., Fu D. T., Chan Y. S., Leung S., Chung S. S. and Chung S. K. (2003) Transgenic mice overexpressing aldose reductase in Schwann cells show more severe nerve conduction velocity deficit and oxidative stress under hyperglycemic stress. *Mol. Cell Neurosci.* **23**, 638–647.

Srivastava S., Chandra A., Bhatnagar A., Srivastava S. K. and Ansari N. H. (1995) Lipid peroxidation product, 4-hydroxynonenal and its conjugate with GSH are excellent substrates of bovine lens aldose reductase. *Biochem. Biophys. Res. Commun.* **217**, 741–746.

Staels B. and Fruchart J. C. (2005) Therapeutic roles of peroxisome proliferator-activated receptor agonists. *Diabetes* **54**, 2460–2470.

Suzuki K., Koh Y. H., Mizuno H., Hamaoka R. and Taniguchi N. (1998) Overexpression of aldehyde reductase protects PC12 cells from cytotoxicity of methylglyoxal or 3-deoxyglucosone. *J. Biochem.* **123**, 353–357.

Suzuki T., Mizuno K., Yashima S., Watanabe K., Taniko K., Suzuki T. and Yabe-Nishimura C. (1999) Characterization of polyol pathway in Schwann cells isolated from adult rat sciatic nerves. *J. Neurosci. Res.* **57**, 495–503.

Suzuki Y., Taniyama M., Muramatsu T., Higuchi S., Ohta S., Atsumi Y. and Matsuoka K. (2004) ALDH2/ADH2 polymorphism associated with vasculopathy and neuropathy in type 2 diabetes. *Alcohol Clin. Exp. Res.* **28**: 111S–116S.

Takagi Y., Kashiwagi A., Tanaka Y., Maegawa H. and Shigeta Y. (1995) Significance of fructose-induced protein oxidation and formation of advanced glycation end product. *J. Diabetes Complications* **9**, 87–91.

Takahashi M., Lu Y. B., Myint T., Fujii J., Wada Y. and Taniguchi N. (1995) *In vivo* glycation of aldehyde reductase, a major 3-deoxyglucosone reducing enzyme: identification of glycation sites. *Biochemistry* **34**, 1433–1438.

Tomlinson D. R. (1999) Role of aldose reductase inhibitors in the treatment of diabetic polyneuropathy, in *Diabetic Neuropathy* (Dyck, P. J., and Thomas, P. K., eds), pp. 330–340. W. B. Saunders, Philadelphia.

Vander Jagt D. L., Robinson B., Taylor K. K. and Hunsaker L. A. (1992) Reduction of trioses by NADPH-dependent aldo–keto reductases. Aldose reductase, methylglyoxal, and diabetic complications. *J. Biol. Chem.* **267**, 4364–4369.

Warming S., Liu P., Suzuki T., Akagi K., Lindtner S., Pavlakis G. N., Jenkins N. A. and Copeland N. G. (2003) Evi3, a common retroviral integration site in murine B-cell lymphoma, encodes an EBFAZ-related Kruppel-like zinc finger protein. *Blood* **101**, 1934–1940.

Watabe K., Fukuda T., Tanaka J., Honda H., Toyohara K. and Sakai O. (1995) Spontaneously immortalized adult mouse Schwann cells secrete autocrine and paracrine growth-promoting activities. *J. Neurosci. Res.* **41**, 279–290.

Watabe K., Ida H., Uehara K. *et al.* (2001) Establishment and characterization of immortalized Schwann cells from murine model of Niemann–Pick disease type C (spm/spm). *J. Peripher. Nerv. Syst.* **6**, 85–94.

Watabe K., Sakamoto T., Kawazoe Y., Michikawa M., Miyamoto K., Yamamura T., Saya H. and Araki N. (2003) Tissue culture methods to study neurological disorders: establishment of immortalized Schwann cells from murine disease models. *Neuropathology* **23**, 68–78.

Yabe-Nishimura C. (1998) Aldose reductase in glucose toxicity: a potential target for the prevention of diabetic complications. *Pharmacol. Rev.* **50**, 21–33.

Yasuda H., Terada M., Maeda K., Kogawa S., Sanada M., Haneda M., Kashiwagi A. and Kikkawa R. (2003) Diabetic neuropathy and nerve regeneration. *Prog. Neurobiol.* **69**, 229–285.

Yoshida K., Shimizugawa T., Ono M. and Furukawa H. (2002) Angiopoietin-like protein 4 is a potent hyperlipidemia-inducing factor in mice and inhibitor of lipoprotein lipase. *J. Lipid Res.* **43**, 1770–1772.

Jikeikai Med J 2006 ; 53 : 55-62

Successful Transduction of Mammalian Astrocytes and Oligodendrocytes by "Pseudotyped" Baculovirus Vector *in Vitro* and *in Vivo*

Hiroshi KOBAYASHI[1,2], Kazuhiko WATABE[3], Sayoko IZUKA[1], Hideki TANI[4], Yoshiharu MATSUURA[4], James BARSOUM[5], Campbell KAYNOR[5], Toya OHASHI[1,2], and Yoshikatsu ETOH[1,2]

[1]*Department of Gene Therapy, Institute of DNA Medicine, The Jikei University School of Medicine*
[2]*Department of Pediatrics, The Jikei University School of Medicine*
[3]*Department of Molecular Neuropathology, Tokyo Metropolitan Institute for Neuroscience*
[4]*Research Center for Emerging Infectious Diseases, Research Institute for Microbial Diseases, Osaka University*
[5]*Biogen, Inc.*

ABSTRACT

Baculovirus vectors can efficiently transduce human hepatoma cells and primary hepatocytes in culture. We report the potential use of baculovirus as a vector for gene delivery into cells of the mammalian central nervous system. We generated a "pseudotyped" baculovirus encoding the bacterial β-galactosidase (β-Gal) gene (LacZ), under the control of the cytomegalovirus promoter, and the vesicular stomatitis virus G protein gene, under the control of the polyhedrin promoter. This virus was used to infect primary cultures of rat glial cells. Three days after infection, these cells were immunostained for β-Gal, glial fibrillary acidic protein (for astrocytes), or galactocerebroside (for oligodendrocytes) to identify the infected cell types. Positive β-Gal immunofluorescence was observed in 10.4% of glial fibrillary acidic protein-positive cells and 35.6% of galactocerebroside-positive cells at a multiplicity of infection of 50. When the virus was injected into adult mouse striatum, β-Gal-positive cells were demonstrated, and no cytological or histological evidence of cell damage, inflammation, or cell infiltration was observed after infection. These findings suggest that baculovirus-mediated gene transfer can be used for gene therapy against nervous system diseases, especially demyelinating disorders, affecting mainly oligodendrocytes. (Jikeikai Med J 2006 ; 53 : 55-62)

Key words : baculovirus, gene therapy, pseudotype, astrocytes, oligodendrocytes

INTRODUCTION

The baculovirus vector has been widely used to obtain high levels of expression of foreign genes under the control of the strong baculoviral promoter (polyhedrin promoter) in insect cells[1]. Although its host specificity had been thought to be restricted to insect cells, the recombinant baculovirus was recently shown to be capable of transferring and expressing foreign genes in mammalian cells, such as hepatocytes[2,3] and nonhepatic cell lines[4]. For the original baculovirus vector the foreign gene is cloned next to the viral polyhedrin promoter, whereas for the recombinant baculovirus the gene is fused to a mammalian pro-

Received for publication, January 6, 2006
小林 博司，渡部 和彦，飯塚佐代子，谷 英樹，松浦 善治，James Barsoum, Campbell Kaynor, 大橋 十也，衛藤 義勝
Mailing address : Hiroshi KOBAYASHI, Department of Gene Therapy, Institute of DNA Medicine, The Jikei University School of Medicine, 3-5-28, Nishi-Shimbashi, Minato-ku, Tokyo 105-8461, Japan.
E-mail address : hr-kb@wd6.so-net.ne.jp

moter, such as cytomegalovirus immediate early promoter and inserted. Efficient gene transfer has been reported, and no viral DNA replication has been observed in mammalian cells. These results suggest that this virus system would be safe for humans.

Sarkis et al. have reported that the baculovirus vector can be used to transfer a marker gene to neurons and astrocytes *in vitro* and *in vivo*[5]. They have reported efficient gene transfer into astrocytes and neurons, but not into oligodendrocytes. Oligodendrocytes are the cells mainly affected in several neurological diseases, such as demyelinating disorders; therefore, for gene therapy in these diseases, investigating ways to transfer genes into oligodendrocytes is important. Barsoum et al. have reported that pseudotype baculovirus, expressing vesiculostomatitis virus G (VSVG) protein in its envelope, transduces mammalian cells much more efficiently than does nonpseudotype baculovirus[6]. In this study, we examined the ability of a pseudotype baculovirus vector to transfer a marker gene in central nervous system (CNS) cells, including oligodendrocytes.

MATERIAL AND METHODS

1. *Construction of pseudotype transfer plasmids*

The pseudotype baculovirus transfer vector, pCZPG (Fig. 1), was generated by inserting expression cassettes encoding the VSVG protein and bacterial β-galactosidase (β-Gal) gene (LacZ) into the standard baculovirus transfer vector BacPak9 (Clontech Laboratories, Inc., Palo Alto, CA, USA)[6]. First, the VSVG gene complementary DNA was excised from the plasmid pLGRNL[7]. This fragment was inserted into the *Bam*HI site of BacPak9, in a direct orientation with respect to the polyhedrin promoter, to create VSVG/BP9. Next, the LacZ gene preceded by the cytomegalovirus promoter and followed by the SV40 poly(A) signal was inserted into VSVG/BP9 such that the LacZ cassette was downstream from the VSVG gene and the direction of transcription was convergent[6].

2. *Pseudotype baculovirus production*

Cells of the insect cell line Sf9 were grown in TC-100 medium (GIBCO/Invitrogen, Carlsbad, CA, USA) with 0.26% Bacto tryptose phosphate broth (Difco, Detroit, MI, USA), 100 μg/ml kanamycin, and 10% fetal bovine serum (GIBCO/Invitrogen). Recombinant pseudotype baculovirus, CZPG, was generated by homologous recombination, as described previously[4,9]. Briefly, pCZPG and the *Bsu* 36I-digested baculovirus genomic DNA were cotransfected into Sf9 cells by lipofectin (GIBCO/Invitrogen). Two days later, the culture medium was harvested and used to infect Sf9 cells in a standard plaque assay. The plaques were isolated and purified by a second round of plaque isolation. After the presence of the predicted recombinant DNA restriction digestion pattern was determined, selected plaques were expanded twice in tissue culture flasks and then on a large scale in 100-ml spinner cultures to obtain a significant volume of virus preparation. The viral titer was determined with a plaque assay[10]. To purify the virus, conditioned media of Sf9 cells infected with the virus were harvested 3 days after infection, and cell debris was removed by centrifugation at 6,000 g for 15

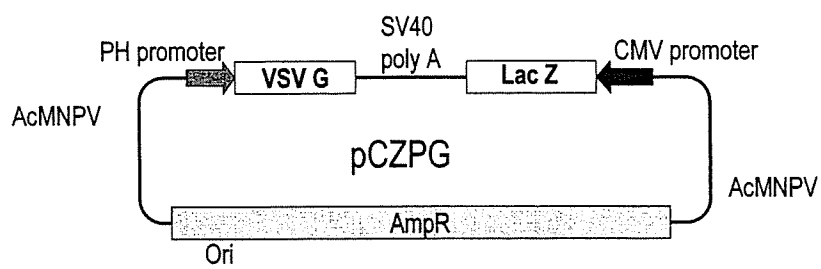

Fig. 1. Structure of pseudotype baculovirus transfer plasmid (pCZPG). AcNMPV, Baculovirus sequences; PH, polyhedrin promoter; AmpR, ampicillin-registance gene; Ori, replication origin; VSVG, Vesicular stomataitis virus G protein gene.

minutes at 4°C. The virus was pelleted by ultracentrifugation at 80,000 g (RPS27-2 rotor, Hitachi, Tokyo) for 90 minutes and resuspended in 1 ml of phosphate buffered saline (PBS), loaded on 10% to 60% (w/v) sucrose gradients, and ultracentrifuged at 77,600 g (P-40ST rotor, Hitachi) for 90 minutes. The virus band was collected and resuspended in PBS and ultracentrifuged at 77,600 for 90 minutes. The virus pellet was resuspended in PBS, and infectious titers were determined with a plaque assay[4].

3. Mixed glial cell culture

Cultures of rat astrocytes and oligodendrocytes were established with the enzyme digestion-Percoll (Pharmacia, Uppsala, Sweden) density gradient method[11-13]. The brains of 10-week-old male Wistar rats were minced and incubated in 0.25% trypsin and 20 μg/ml DNase in calcium- and magnesium-free Hanks balanced salt solution (HBSS) for 40 minutes at 37°C. Dissociated cells were passed through a 100-μm nylon mesh. Isolated cells suspended in HBSS were mixed with Percoll, and a gradient was formed by centrifugation for 25 minutes at 15,000 g in a high-speed refrigerated centrifuge with a fixed-angle rotor (Hitachi). The final concentration of Percoll was 30% in HBSS. An astrocyte- and oligodendrocyte-enriched fraction, bound by an upper myelin layer and a lower erythrocyte layer, was collected and diluted in three volumes of HBSS, before being harvesting by low-speed centrifugation for 10 minutes. The cells were washed twice in HBSS, suspended in feeding medium (1×10^5 cells/ml), and seeded on polysine-coated 9-mm-diameter round coverslips (Aclar, Honeywell/AlliedSignal, Pottsville, PA, USA). The feeding medium consisted of 5% fetal bovine serum, 50 units/ml penicillin, and 50 μg/ml streptomycin in Isocove's modified Dulbecco's minimum essential medium. The cultures were maintained in 5% CO_2 at 37°C for 2 weeks, with the culture medium being changed every 4 days.

4. Infection of glial cell cultures with CZPG

Living cells of mixed rat glial cultures on coverslips after 2 weeks in vitro were infected with a 10-μl solution of purified CZPG at a multiplicity of infection of 50 for 1 hour and were incubated in feeding medium for 3 days in 5% CO_2 at 37°C. To detect β-Gal expression in infected cells, immunofluorescence was performed with a rabbit antibody to β-Gal. Cell types were identified with immunofluorescence using antibodies to glial fibrillary acidic protein (GFAP) and galactocerebroside (GC), specific markers for astrocytes and oligodendrocytes, respectively. For double immunofluorescence staining for β-Gal and GFAP, cells on coverslips were fixed in 1% paraformaldehyde in PBS for 10 minutes at 4°C and in methanol for 10 minutes at −20°C and incubated at room temperature for 1 hour with a mixture of a rabbit antibody to β-Gal (Eppendorf-5 Prime, Boulder, CO, USA) and rat monoclonal antibody (hybridoma soup) to GFAP[14] (kindly provided by Dr. Seung U. Kim, University of British Columbia) at final dilutions of 1 : 50 and 1 : 2, respectively. This incubation was followed by incubation at room temperature for 1 hour with a mixture of fluorescein isothiocyanate (FITC)-conjugated goat anti-rabbit IgG (Cappel, MP Biomedicals, Aurora, OH, USA) and rhodamine-conjugated goat anti-rat IgG (Cappel) at a final dilution of 1 : 50. For double immunofluorescence staining for β-Gal and GC, living cells on coverslips were incubated with mouse monoclonal antibody (hybridoma soup) to GC[15] (kindly provided by Dr. Seung U. Kim) at a dilution of 1 : 2 for 30 minutes at room temperature. After being washed with Isocove's modified Dulbecco's minimum essential medium, the cells were incubated with rhodamine-conjugated goat anti-mouse IgG (Cappel) at a final dilution of 1 : 50 for 30 minutes at room temperature. The cells were fixed with 1% paraformaldehyde in PBS at 4°C for 10 minutes and cold methanol at −20°C for 10 minutes. After being washed in PBS, the cells were incubated with rabbit antibody to β-Gal at a dilution of 1 : 50 for 1 hour at room temperature. After being washed, the cells were incubated with FITC-conjugated goat anti-rabbit IgG at a final dilution of 1 : 50 for 45 minutes at room temperature. After being washed, coverslips were mounted on glass slides with 20% glycerol/10% polyvinylalcohol in 0.1 M Tris-HCl buffer, pH 8.0. Cells were then examined under a universal microscope (Olympus Opti-

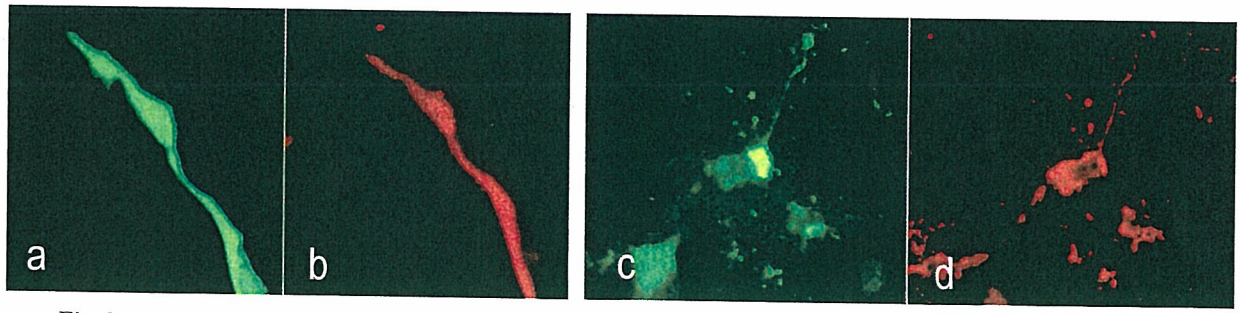

Fig. 2. β-Gal expression in rat primary culture astrocytes and oligodendrocytes *in vitro*. a, b: Astrocytes infected with CZPG *in vitro* for 3 days. β-Gal-FITC (a) and GFAP- rhodamine (b) double immunofluorescence. c, d: Oligodendrocytes infected with CZPG *in vitro* for 3 days. β-Gal-FITC (c) and GC-rhodamine (d) double immunofluorescence.

cal Co., Tokyo) equipped with fluorescein and rhodamine optics.

5. Infection of mouse brains with CZPG

Intracerebral injection of purified CZPG was carried out as follows: 6- to 8-week-old normal female C57BL/6 mice ($n=12$) were anesthetized with intraperitoneal injection of 40 mg/kg of pentobarbital sodium. Five microliters of purified CZPG (1×10^9 pfu/ml) was injected slowly into the left striatum (AP: to 1 mm; ML: 2 mm; DV: 3.6 mm to the bregma) or the ventricle (AP: to 1 mm; ML: 2 mm; DV: 2.6 mm to the bregma) through a syringe (Hamilton Co., Reno, NV, USA). Three days after the operation, the mice were deeply anesthetized through inhalation of diethyl ether and intracardially perfused with 4% paraformaldehyde in PBS. The brains were removed, postfixed in the same fixative for 24 hours, and cryoprotected in 30% sucrose in PBS, after which 20-μm-thick coronal sections were cut with a cryostat. Gene transfer into the CNS was identified with β-Gal staining. These sections were washed four times in PBS and stained in a solution of 1 mg/ml X-gal (5-bromo-4-chloro-3-indolyl-β-D-galactopyranoside), 5 mM $K_3Fe(CN)_6$, 5 mM $K_4Fe(CN)_6$, and 2 mM $MgCl_2$ in PBS[16]. Cell types were identified with immunofluorescence using antibodies to GFAP and 3′,5′-cyclic nucleotide phosphodiesterase (CNP) for astrocytes and oligodendrocytes, respectively. The sections were washed in PBS and incubated in 0.1% Triton X-100 in PBS (PBST) for 30 minutes and in 3% normal goat serum in PBST for 1 hour at room temperature. For double immunofluorescence staining for β-Gal and GFAP, the sections were incubated at 4°C overnight with a mixture of rabbit antibody to β-Gal and rat monoclonal antibody to GFAP at final dilutions of 1 : 50 and 1 : 2, respectively. This incubation was followed by incubation at room temperature for 1 hour with a mixture of FITC-conjugated goat anti-rabbit IgG and rhodamine-conjugated goat anti-rat IgG at a final dilution of 1 : 50. For double immunofluorescence staining for β-Gal and CNP, the sections were incubated at 4°C for 12 hours with a mixture of rabbit antibody to β-Gal and mouse monoclonal antibody to CNP at final dilutions of 1 : 50 and 1 : 100, respectively. This incubation was followed by incubation at room temperature for 1 hour with a mixture of FITC-conjugated anti-rabbit IgG and rhodamine-conjugated anti-mouse IgG at a final dilution of 1 : 50.

RESULTS

1. Transduction of cultured glial cells by CZPG

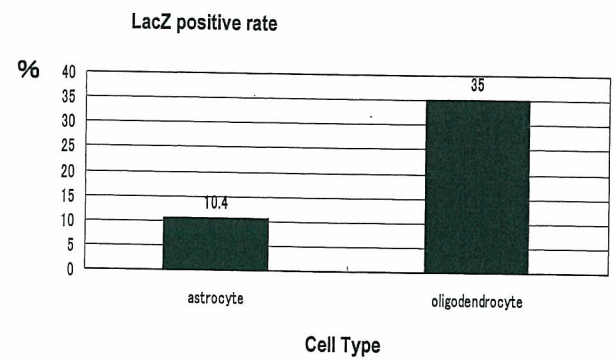

Fig. 3. Efficiency of LacZ gene transfer into rat primary culture *in vitro*.

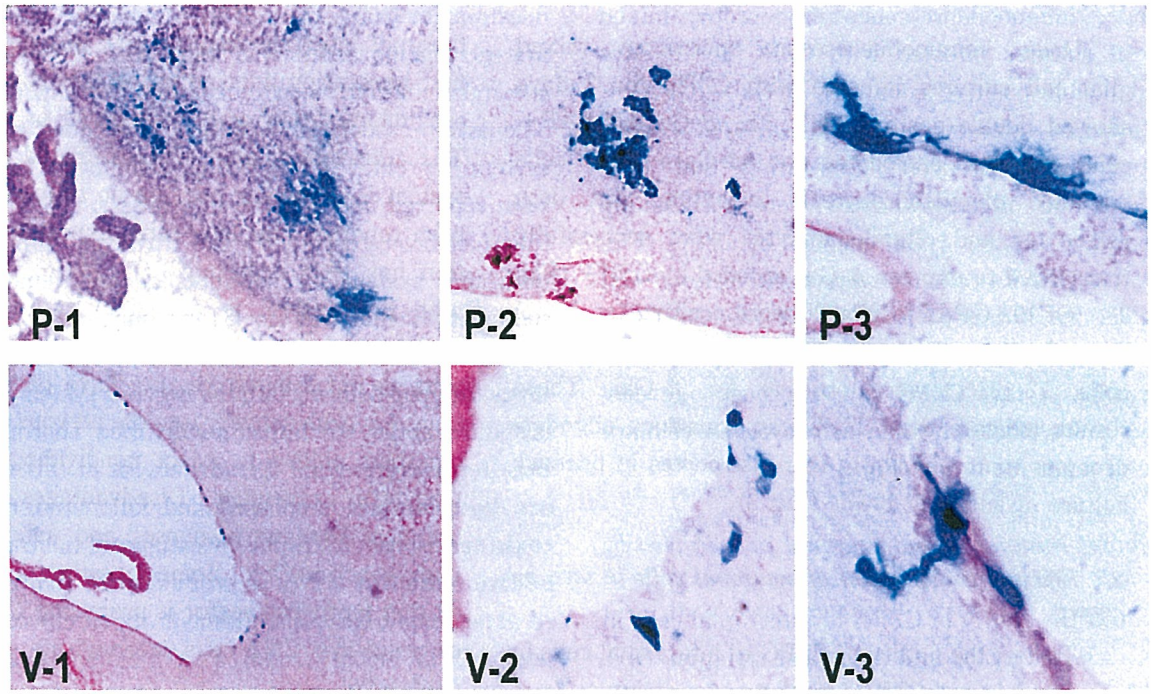

Fig. 4. β-Gal expression in normal mouse brain *in vivo*. 3 days after injection of CZPG into normal mouse (C57BL/6) striatum, gene transfer into CNS *in vivo* was identified by β-Gal staining.
P1-P3 ; the slides of the mouse brain injected in the parenchyma. Lac Z positive cells were seen in near the choroid plexus (P-1), striatum (P-2), and corpus callosum (P-3).
V1-V3 ; the slides of the mouse brain injected in the ventricle. Lac Z positive cells were seen in the ependimal cell (V-1, 2) and partially migrated into the parenchyma (V-3).

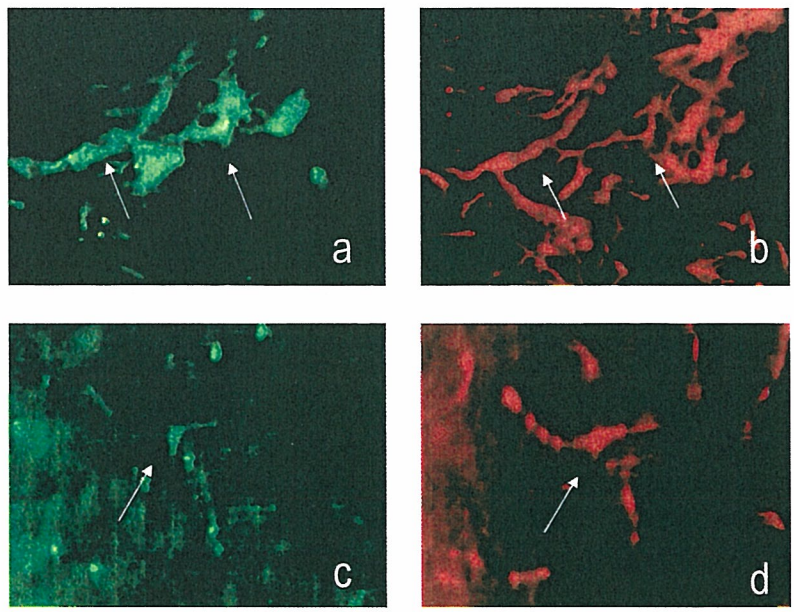

Fig. 5. The slides of the Immunohistochemistry of the mouse brain injected in the parenchyma, double-positive cells, i.e. β-Gal+/GFAP+ (an infected astrocytes ; a, b) and β-Gal+/CNP+ (infected oligodendrocyte : c, d) cells were demonstrated by double immunofluorescence microscopy, indicating both astrocytes and oligodendrocytes can also be transduced *in vivo* by CZPG.

Under immunofluorescence microscopy, mixed glial cell cultures infected with CZPG for 3 days showed double-positive cells, i.e., β-Gal+/GFAP+ cells (infected astrocyte) and β-Gal+/GC+ cells (infected oligodendrocytes), indicating that both astrocytes and oligodendrocytes were successfully transduced to express β-Gal encoded by CZPG (Fig. 2). Of 192 GFAP+cells, 20 were positive for β-Gal (transduction efficiency; 10.4%). Of the 202 GC+ cells, 72 (35%) were positive for β-Gal. These results indicate that CZPG can transduce oligodendrocytes more efficiently than astrocytes in primary culture of adult rat brain (Fig. 3).

2. Efficient transduction of neuronal cells in vivo by CZPG

To test the ability of CZPG to infect glial cells in vivo, we injected CZPG into the mouse striatum ($n=12$). Three days after injection, β-Gal positive cells were demonstrated in the parenchyma (Fig. 4 P1, P2, P3) and periventricular zone (Fig. 4 V1, V2, V3). We detected transduction mainly for parenchymal cells (P1, P2, P3) and ependymal cells (V1, V2), partially migrated into the parenchyma (V3). Next, we tried immunohistochemistry *in vivo*, double-positive cells, i.e., β-Gal+/GFAP+ cells (infected astrocytes) and β-Gal+/CNP+ cells (infected oligodendrocytes) were demonstrated by double immunofluorescence microscopy, indicating that both astrocytes and oligodendrocytes can also be transduced *in vivo* by CZPG (Fig. 5). We observed no cytological damage *in vitro* and no histological evidence of cell damage, inflammation, or cell infiltration after infection with CZPG.

DISCUSSION

Gene therapy for neurological disorders requires an efficient and stable gene delivery system for the CNS. As for gene transfer systems into the CNS cells, adenovirus, adeno-associated virus (AAV), herpesvirus, and lentivirus vectors have been studied[17]. Although adenovirus vector has been reported to be a useful gene transfer system for the nervous system[18–20], its expression is transient because the vector does not integrate into the host genome. Moreove first-generation adenovirus vectors cause severe tissue inflammation when inoculated in brain tissue[21]. The adeno-associated virus-mediated gene transfer system is promising because no cellular toxicity has been reported and long-term expression by integration has been reported[20,22,23]. However, a problem with this system is the difficulty of preparing a sufficiently large virus stock for clinical use. Herpes simplex virus-based vectors have particular advantages for gene delivery into the nervous system including their ability to infect nondividing neurons and long-term expression. Disadvantages of this system are host immune responses and inflammatory and toxic reactions[24,25]. Some investigators have reported that lentivirus vector is promising for the transfer of genes into CNS cells, although its safety rema unclear[26,27].

To seek an alternative approach to overcome the limitations of current vector systems for transducing CNS cells, we tested a baculovirusmediated gene transfer system in rodent CNS cells in vivo and in vitro. The generation of recombinant baculovirus is relatively less time-consuming, and expansion of the virus stock is relatively easy. The titer of the virus stock after purification is high and comparable to that of adenovirus. Large DNA (up to 15 kb) can be inserted into the transfer vector. Moreover, baculovirus cannot replicate in mammalian cells, and no cell toxicity has been observed[28]. In fact, there was no evidence of tissue inflammation or cell damage in the present study.

The first attempt to transfer genes to mammal cells with the baculovirus vector was reported by Hofman et al. in 1995. They successfully transferred a gene to mammalian hepatocytes. However, they failed to transfer genes to neural cell lines, such as mouse neuroblastoma Neuro-2a and human astrocytoma SW 1088[2]. Recently, Sarkis et al. have reported successful transduction of nervous system cells (both neurons and astrocytes) *in vitro* and *in vivo* using nonpseudotype baculovirus[5]. In the present study, we used a pseudotype vector. By pseudotyping, the VSVG protein is expressed in the viral envelope and mediates the escape of the recom-

binant pseudotype baculovirus from the intracellular vesicles. The efficiency of the escape may be the rate-limiting step for transduction[6]. We also tried a nonpseudotype baculoviral vector and detected efficient transduction *in vitro*, especially in the liver cell line Hep G2, but detected no transduction *in vivo* (data not shown). The baculovirus vector CZPG prepared in this study could transduce both astrocytes and oligodendrocytes. This ability implies a potential advantage of pseudotype baculovirus vectors for use in CNS gene therapy, because oligodendrocytes are the cells principally affected in many neurological diseases, such as globoid cell leukodystrophy (Krabbe's disease), metachromatic leukodystrophy, and adrenoleukodystrophy. We are now generating a baculovirus vector expressing galactocerebrosidase, which is lacking in Krabbe's disease, to investigate its therapeutic effects in a mouse model of Krabbe's disease. Our failure to find cytological or histological evidence of cell damage, inflammation, or cell infiltration after infection of CZPG *in vitro* and *in vivo* point is also important for gene transfer into CNS and other organ systems *in vivo*.

There are several unanswered questions regarding our baculovirus vector system; i.e., how long the expression persists and how efficiently it infects oligodendrocytes *in vivo*. For the treatment of Krabbe's disease, highly efficient transduction of oligodendrocytes and persistent expression of transferred genes will be required. Additional experiments are underway to answer these questions.

References

1. Luchow VA, Summers MD. Trends in the development of baculovirus expression vectors. Biotechnology 1988; 6: 47-55.
2. Hofmann C, Sandig V, Jennings G, Rudolph M, Schlag P, Strauss M. Efficient gene transfer into human hepatocytes by baculovirus vectors. Proc Natl Acad Sci USA 1995; 92: 10099-103.
3. Sandig V, Hofmann C, Steinert S, Jennings G, Schlag P, Strauss M. Gene transfer into hepatocytes and human liver tissue by baculovirus vectors. Hum Gene Ther 1996; 7: 1937-45.
4. Shoji I, Aizaki H, Tani H, Ishii K, Chiba T, Saito I, et al. Efficient gene transfer into various mammalian cells, including non-hepatic cells, by baculovirus vectors. J Gen Virol 1997; 78: 2657-64.
5. Sarkis C, Seguera C, Petres S, Buchet D, Ridet JL, Edrlman L, et al. Efficient transduction of neural cells *in vitro* and *in vivo* by a baculovirus-derived vector. Proc Natl Acad Sci USA 2000; 97: 14638-43.
6. Barsoum J, Brown R, McKee M, Boyce FM. Efficient transduction of mammalian cells by a recombinant baculovirus having vesicular stomatitis virus G glycoprotein. Hum Gene Ther 1997; 8: 2011-18.
7. Burns JC, Friedmann T, Driever W, Burrascano M, Yee JK. Vesicular stomatitis virus G glycoprotein pseudotyped retroviral vectors: concentration to very high titer and efficient gene transfer into mammalian and nonmammalian cells. Proc Natl Acad Sci USA 1993; 90: 8033-7.
8. Boyce FM, Bucher NL. Baculovirus-mediated gene transfer into mammalian cells. Proc Natl Acad Sci USA 1996; 93: 2348-52.
9. Matsuura Y, Possee RD, Overton HA, Bishop DHL. Baculovirus expression vectors: the requirements for high level expression of proteins, including glycoproteins. J Gen Virol 1987; 68: 1233-50.
10. O'Reilly DR, Miller LK, Luckow VA. Freeman WH, editer. Baculovirus expression vectors: a laboratory manual. New York: Oxford University Press; 1992.
11. Kim SU, Sato Y, Silberberg DH, Pleasure DE, Rorke LB. Long-term culture of human oligodendrocytes: isolation, growth and identification. J Neurol Sci 1983; 62: 295-301.
12. Kim SU. Antigen expression by glial cells grown in culture. J Neuroimmunol 1985; 8: 255-82.
13. Watabe K, Osborne D, Kim SU. Phagocytic activity of human adult astrocytes and oligodendrocytes in culture. J Neuropathol Exp Neurol 1989; 48: 499-506.
14. Lee WMY, Page CD, Wu HL, Schlaepfer WW. Monoclonal antibodies to gel-excised glial filament protein and their reactivities with other intermediate filament proteins. J Neurochem 1984; 42: 25-32.
15. Ranscht B, Clapshaw PA, Price I, Noble M, Seifert W. Development of oligodendrocytes and Schwann cells studied with a monoclonal antibody against galactocerebroside. Proc Natl Acad Sci USA 1982; 79: 2709-13.
16. Scholer HR, Balling R, Hatzopoulos AK, Suzuki N, Gruss P. Octamer binding proteins confer transcriptional activity in early mouse embryogenesis. EMBO J 1989; 8: 2551-7.
17. Bjorklund A, Kirik D, Rosenblad C, Georgievska B, Lundberg C, Mandel RJ. Towards a neuroprotective gene therapy for Parkinson's disease: use of adenovirus, AAV and lentivirus vectors for gene transfer of GDNF to the nigrostriatal system in the rat parkinson model. Brain Res 2000; 886: 82-98.
18. Parkis RJ. Improvements in adenoviral vector technology: overcoming barriers for gene therapy. Clin Genet 2000; 58: 1-11.

19. Russel WC. Update on adenovirus and its vectors. J Gen Virol 2000; 81: 2573-604.
20. Gaetano R, Pietro M, Carmen P, Anttonio G. Latest developments in gene transfer technology: achievements, perspectives, and controversies over therapeutic applications. Stem Cells 2000; 18: 19-39.
21. Le Gal La Salle G., Robert JJ, Bernard S, Ridoux V, Stratford-Perricaudet LD, Perricaudet M, et al. An adenovirus vector for gene transfer into neurons and glia in the brain. Science 1993; 259: 988-90.
22. Athenasopoulos T, Fabb S, Dickson G. Gene therapy based on adeno-associated virus: characteristics and applications to acquired and inherited disease. Int J Mol Med 2000; 6: 363-75.
23. Monahan PE, Samulski RJ. AAV vectors: is clinical success on the horizon? Gene Ther 2000; 7: 24-30.
24. Hammercchmidt W. Herpesvirus vectors come of age. Curr Opin Mol Ther 2000; 5: 532-9.
25. Latchman DS. Gene therapy with herpes simplex virus vectors: progress and prospects for clinical neuroscience. Neuroscientist 2001; 7: 528-37.
26. Lamothe B, Joshi S. Current developments and future prospectives for HIV gene therapy using interfering RNA-based strategies. Front Biosci 2000; 1: D527-55.
27. Miyoshi H, Smith KA, Mosier DE, Verma IM, Torbett TE. Transduction of human CD34+ cells that mediate long-term engraftment of NOD/SCID mouse by HIV vectors. Science 1999; 283: 682-6.
28. Bishop DHL, Entwistle PF, Cameron IR, Allen CJ, Posser RD. Field trial of genetically engineered baculovirus insecticides: the release of genetically engineered organisms. Sussman M, Collins CH, Skinner FA, Stewart-Tull DE, editors. London; Academic Press: 1988; p. 143-79.

BRAIN RESEARCH 1111 (2006) 187–195

available at www.sciencedirect.com

ScienceDirect

www.elsevier.com/locate/brainres

BRAIN RESEARCH

Research Report

Adenoviral gene transfer of hepatocyte growth factor prevents death of injured adult motoneurons after peripheral nerve avulsion

Yuichi Hayashi[a,b], Yoko Kawazoe[a], Tsuyoshi Sakamoto[a], Miyoko Ojima[a], Wei Wang[a], Takanori Takazawa[a], Daisuke Miyazawa[c], Wakana Ohya[c], Hiroshi Funakoshi[c], Toshikazu Nakamura[c], Kazuhiko Watabe[a,*]

[a]Department of Molecular Neuropathology, Tokyo Metropolitan Institute for Neuroscience, Tokyo Metropolitan Organization for Medical Research, 2-6 Musashidai, Fuchu, Tokyo 183-8526, Japan
[b]Department of Neurology and Geriatrics, Gifu University Graduate School of Medicine, 1-1 Yanagido, Gifu 501-1194, Japan
[c]Division of Molecular Regenerative Medicine, Department of Biochemistry and Molecular Biology, Osaka University Graduate School of Medicine, B-7, Suita, Osaka 565-0871, Japan

ARTICLE INFO

Article history:
Accepted 27 June 2006
Available online 1 August 2006

Keywords:
Adult rat
Avulsion
Facial nerve
Hepatocyte growth factor
Motoneuron
Spinal nerve

ABSTRACT

Hepatocyte growth factor (HGF) exhibits strong neurotrophic activities on motoneurons both in vitro and in vivo. We examined survival-promoting effects of an adenoviral vector encoding human HGF (AxCAhHGF) on injured adult rat motoneurons after peripheral nerve avulsion. The production of HGF in COS1 cells infected with AxCAhHGF and its bioactivity were confirmed by ELISA, Western blot and Madin-Darby canine kidney (MDCK) cell scatter assay. The facial nerve or the seventh cervical segment (C7) ventral and dorsal roots of 3-month-old Fischer 344 male rats were then avulsed and removed from the stylomastoid or vertebral foramen, respectively, and AxCAhHGF, AxCALacZ (adenovirus encoding β-galactosidase gene) or phosphate-buffered saline (PBS) was inoculated in the lesioned foramen. Treatment with AxCAhHGF after avulsion significantly prevented the loss of injured facial and C7 ventral motoneurons as compared to AxCALacZ or PBS treatment and ameliorated choline acetyltransferase immunoreactivity in these neurons. These results indicate that HGF may prevent the degeneration of motoneurons in adult humans with motoneuron injury and motor neuron diseases.

1. Introduction

Hepatocyte growth factor (HGF) was initially identified and purified as a potent mitogen of primary cultured hepatocytes (Nakamura et al., 1984, 1989). HGF is a heterodimeric protein composed of α and β chains and induces proliferation, migration, differentiation of target cells as well as organogenesis and neovascularization (Funakoshi and Nakamura, 2003). In the nervous system, HGF exhibits strong neurotrophic activities for motoneurons both in vitro and in vivo (Caton et al., 2000; Ebens et al., 1996; Funakoshi and Nakamura, 2003; Honda et al., 1995; Koyama et al., 2003, Maina and Klein, 1999; Naeem et al., 2002; Novak et al., 2000; Okura et al., 1999; Sun et al., 2002; Wong et al., 1997; Yamamoto et al., 1997). There have

* Corresponding author. Fax: +81 42 321 8678.
E-mail address: kazwtb@tmin.ac.jp (K. Watabe).

0006-8993/$ – see front matter © 2006 Elsevier B.V. All rights reserved.
doi:10.1016/j.brainres.2006.06.104

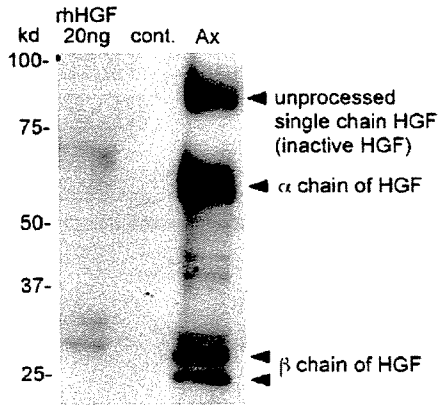

Fig. 1 – Western blot analysis of conditioned media (CMs) obtained from COS1 cells uninfected (cont.) or infected (Ax) with AxCAhHGF. The CMs harvested at 3 days after infection were concentrated by heparin beads, electrophoresed, blotted and immunolabeled for HGF as described in the text.

been no reports, however, concerning the neurotrophic effects of HGF on adult motoneuron death after proximal nerve injury. In animal models of adult motoneuron injury, avulsion of cranial and spinal nerves causes marked motoneuron degeneration in adult rats (Koliatsos et al., 1994; Moran and Graeber, 2004; Ruan et al., 1995; Sakamoto et al., 2000, 2003a, 2003b; Søreide, 1981; Watabe et al., 2000, 2005; Wu, 1993), so that these animal models can be useful for therapeutic evaluation of neurotrophic factors or neuroprotective molecules against adult motoneuron death (Ikeda et al., 2003; Sakamoto et al., 2000, 2003a, 2003b; Watabe et al., 2000, 2005). We have recently shown that adenoviral gene transfer of glial-cell-line-derived neurotrophic factor (GDNF), brain-derived neurotrophic factor (BDNF), transforming growth factor-β2 (TGFβ2) and growth inhibitory factor (GIF)/metallothionein-III (MT-III) prevented the death of adult rat facial and spinal motoneurons after facial nerve and cervical spinal root avulsion (Sakamoto et al., 2000, 2003a, 2003b; Watabe et al., 2000). In the present study, we investigated whether HGF protects injured motoneurons after facial nerve or spinal root avulsion by using a recombinant adenoviral vector encoding human HGF.

2. Results

2.1. *Bioassay of recombinant human HGF*

In this study, we constructed a recombinant adenoviral vector encoding human HGF (AxCAhHGF). To test the ability of AxCAhHGF to induce human HGF expression in vitro, COS1 cells were infected with AxCAhHGF and the conditioned media (CMs) were harvested at 3 days postinfection. The levels of human HGF in uninfected and infected CMs analyzed by enzyme-linked immunosorbent assay (ELISA) were 1.9± 0.4 ng/ml and 2004.8±160 ng/ml, respectively ($n=3$). Western blot analysis of the CM harvested at 3 days postinfection showed immunoreactive bands of α-chain, β-chain and pro-HGF (inactive, unprocessed single chain precursor form) (Fig. 1). The CM obtained from uninfected COS1 cells did not show any immunoreactive bands. The Madin-Darby canine kidney (MDCK) cell scatter assay showed definite bioactivitiy of AxCAhHGF-infected COS1 CM; i.e., the activity of 1:500-diluted CM containing 4 ng/ml HGF as measured by ELISA corresponded to that of 2 ng/ml recombinant human HGF (rhHGF) that induced scattering of MDCK cells (Fig. 2).

2.2. *Adenoviral-vector-mediated HGF gene expression in facial nuclei*

We then examined the expression of adenovirus-mediated HGF in injured motoneurons after avulsion. We have pre-

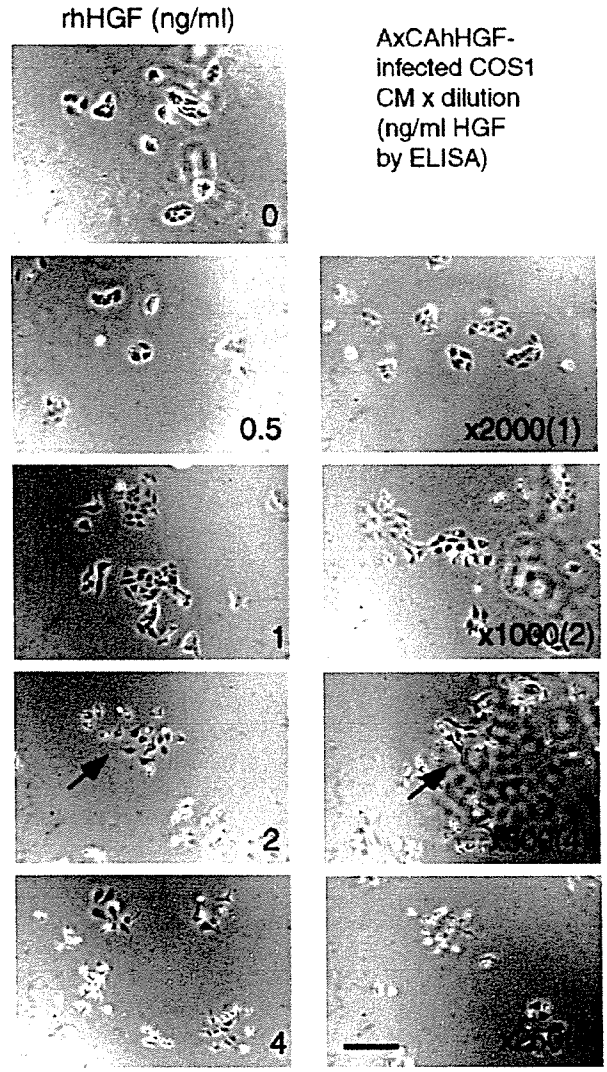

Fig. 2 – Madin-Darby canine kidney (MDCK) cell scatter assay for HGF bioactivity. MDCK cells were cultured in the presence or absence of AxCAhHGF-infected COS1 CM or rhHGF as described in the text. The activity of 1:500-diluted CM containing 4 ng/ml human HGF as measured by ELISA corresponds to that of 2 ng/ml recombinant human HGF that induced scattering of MDCK cells (arrows). Scale bar=50 μm.

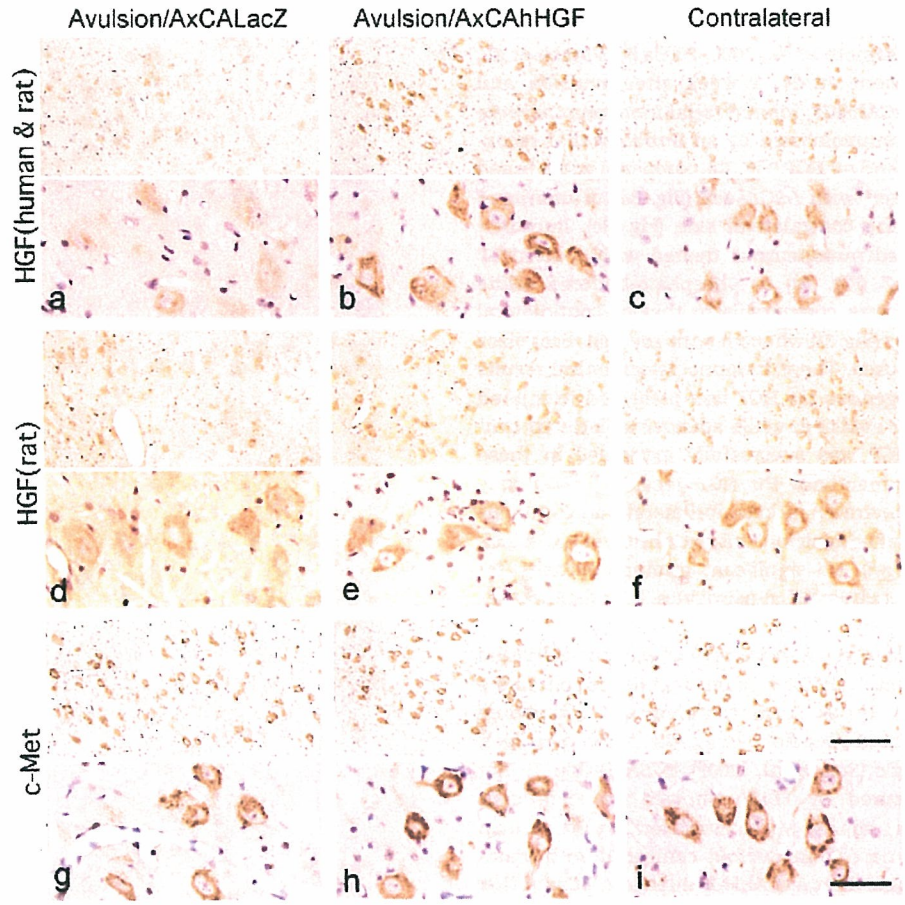

Fig. 3 – Low (top) and high (bottom)-magnified photomicrographs of immunohistochemistry of facial motoneurons at the ipsilateral (a, b, d, e, g, h) and contralateral (c, f, i) sides 7 days after facial nerve avulsion and the treatment with AxCALacZ (a, d, g) or AxCAhHGF (b, c, e, f, h, i) using antibodies against human and rat HGF (a–c), rat HGF (b–f) and c-Met (g–i). Counterstained with hematoxylin. Injured facial motoneurons after avulsion and AxCAhHGF treatment are more intensely immunolabeled by anti-human and rat HGF antibody (b) compared with injured motoneurons with AxCALacZ treatment (a) or contralateral intact motoneurons (c). Immunoreactivity of injured motoneurons treated with AxCALacZ (d) or AxCAhHGF (e) is comparable to that of contralateral intact motoneurons (f) when anti-rat HGF antibody was used. Immunoreactivity for c-Met is consistently demonstrated in both injured and contralateral motoneurons (g–i). Scale bars=200 μm (top), 50 μm (bottom).

viously demonstrated that injured motoneurons and their axons were labeled with X-Gal after facial or seventh cervical segment (C7) avulsion and inoculation of an adenovirus encoding bacterial β-galactosidase gene as a reporter (AxCA-LacZ) into lesioned stylomastoid or vertebral foramen, respectively (Sakamoto et al., 2000; Watabe et al., 2000). This indicates the diffusion of the virus through the facial canal or intervertebral foramen, its adsorption to injured axons, retrograde transport of the virus via intramedullary facial or spinal nerve tracts to soma of the motoneurons and

Table 1 – HGF protein levels in brain stem tissue containing facial nuclei after facial nerve avulsion and treatment with adenoviral vectors

Treatment (n= animal number)	Human HGF (ng/g)		Rat HGF (ng/g)	
	Ipsilateral	Contralateral	Ipsilateral	Contralateral
AxCALacZ (n=3)	u.d.	u.d.	20.3±3.8	17.2±2.3
AxCAhHGF (n=3)	61.8±36.1	13.1±11.4	21.2±3.1	22.8±2.8

Seven days after facial nerve avulsion and the treatment with AxCALacZ or AxCAhHGF, the brain stem tissues containing facial nuclei (10–14 mg wet weight) were examined by human- and rat-specific HGF ELISA. u.d. = under the detection limit (<2.4 ng/g tissue).

successful induction of the virus-induced foreign gene in these neurons (Sakamoto et al., 2000, 2003a,b; Watabe et al., 2000). In the present study, 1 week after avulsion and treatment with AxCAhHGF, injured facial motoneurons were more intensely immunolabeled by an antibody that recognizes both human and rat HGF (Fig. 3b), compared with injured motoneurons treated with AxCALacZ (Fig. 3a) or uninjured motoneurons on the contralateral side (Fig. 3c). Immunoreactivity of injured motoneurons treated with AxCAhHGF (Fig. 3e), AxCALacZ (Fig. 3d) or phosphate-buffered saline (PBS) (not shown) was comparable to that of contralateral intact motoneurons (Fig. 3f) when an antibody that recognizes only rat HGF was used. These immunohistochemical results suggest that endogenous rat HGF was preserved in injured motoneurons after avulsion, while adenovirus-induced exogenous human HGF was successfully expressed in these neurons. Immunoreactivity for HGF receptor c-Met was consistently demonstrated in both ipsilateral and contralateral motoneurons after avulsion and AxCAhHGF or AxCALacZ treatment (Figs. 3g–i). No significant immunoreactivity for HGF and c-Met was observed in astrocytes, oligodendrocytes or microglia.

We further examined the expression of exogenous human HGF and endogenous rat HGF in brain stem tissue containing facial nuclei after facial nerve avulsion and adenovirus treatment by human-specific (Funakoshi and Nakamura, 2003) or rat-specific (Sun et al., 2002) ELISA (Table 1). Rat HGF levels measured by ELISA showed no significant difference between injured and contralateral sides. Human HGF levels were more than twofold compared with endogenous rat HGF levels after AxCAhHGF infection. Human HGF was also detectable in the tissues at the contralateral side after AxCAhHGF infection, which was considered to originate from injured and infected motoneurons at the ipsilateral side (Table 1).

One week after facial nerve avulsion and the treatment with AxCAhHGF, RT-PCR analysis showed that virus-induced human HGF mRNA transcripts were expressed in the brainstem tissue containing the facial nucleus on the ipsilateral, but not the contralateral side, whereas endogenous rat HGF

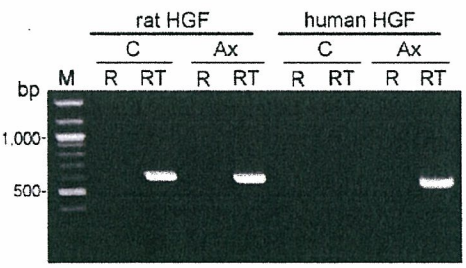

Fig. 4 – RT-PCR analysis of HGF mRNA transcripts in ipsilateral (Ax) and contralateral (C) sides of the brain stem tissue containing facial nuclei 7 days after facial nerve avulsion and AxCAhHGF treatment. The PCRs were performed on RNA without (R) or with (RT) reverse transcription. Primers that amplify rat or human HGF mRNA transcripts were used as described in the text. M=DNA size marker.

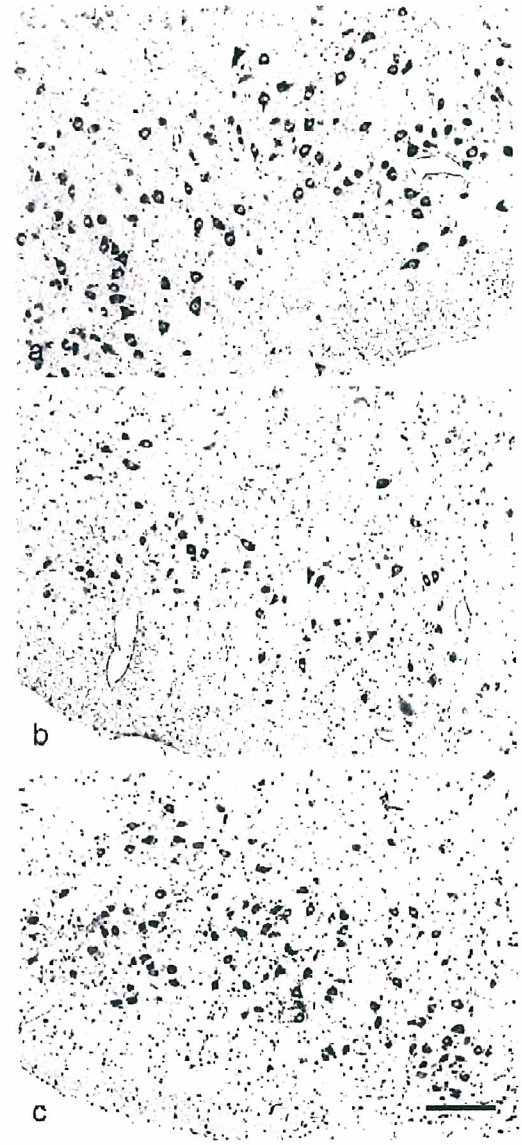

Fig. 5 – Photomicrographs of facial motoneurons at the contralateral (a) and ipsilateral (b, c) side 4 weeks after the right facial nerve avulsion and the treatment of AxCALacZ (b) or AxCAhHGF (c). Pictures (a) and (c) were taken from the same section. Nissl stain. Scale bar=200 μm.

mRNA was consistently detected in the tissues on both ipsilateral and contralateral sides after avulsion (Fig. 4).

2.3. *Neuroprotective effects of HGF gene transfer*

Four weeks after facial nerve or C7 spinal root avulsion and treatment with phosphate-buffered saline (PBS) or AxCALacZ, the number of surviving facial or spinal motoneurons declined to 30–50% of that on the contralateral side as described previously (Sakamoto et al., 2000, 2003a, 2003b; Watabe et al., 2000). The treatment with AxCAhHGF prevented the loss of facial (58.8±5.9% survival) and spinal (75.4±4.4% survival)

motoneurons after avulsion compared with the treatment with PBS (30.2±6.7% survival of facial motoneurons; 44.6±9.3% survival of C7 motoneurons) or AxCALacZ (32.4±4.3% survival of facial motoneurons; 46.0±5.3% survival of C7 motoneurons) (Sakamoto et al., 2000) (Figs. 5, 6; Table 2). The treatment with AxCAhHGF after avulsion attenuated the decrease of choline acetyltransferase (ChAT) immunoreactivity in injured facial motoneurons compared with the treatment with PBS or AxCALacZ (Fig. 7). We found no perivascular or intrathecal lymphocytic/mononuclear cell infiltration in the facial nuclei and the spinal cord tissues that would be histologically defined and identified in case of immunogenic reaction against adenovirus infection (Figs. 5, 6).

Table 2 – Survival of motoneurons after facial nerve and spinal root avulsion and treatment with adenoviral vectors

Treatment (*n*=animal number)	Ipsilateral motoneuron number	Contralateral motoneuron number	% Survival
Facial nerve avulsion			
PBS (*n*=8)	213±41	712±38	30.2±6.7
AxCALacZ (*n*=4)	239±29	741±73	32.4±4.3
AxCAhHGF (*n*=7)	441±87*	745±38	58.8±5.9*
Spinal root avulsion			
PBS (*n*=4)	66±22	144±20	44.6±9.3
AxCALacZ (*n*=4)	69±9	150±12	46.0±5.3
AxCAhHGF (*n*=4)	108±15**	143±14	75.4±4.4**

Numbers of facial motoneurons and the percent survival at the ipsilateral (lesion) side relative to the contralateral (control) side 4 weeks after avulsion and treatment with phosphate-buffered saline (PBS), AxCALacZ and AxCAhHGF. Results are presented as the mean±SD. Statistical comparison was done by Mann–Whitney *U* test. *$P<0.01$ vs. PBS- and AxCALacZ-treated groups. **$P<0.05$ vs. PBS- and AxCALacZ-treated groups.

3. Discussion

HGF binds to tyrosine kinase receptor c-Met and triggers diverse biological responses that include cell motility, proliferation, morphogenesis, neurite extension and anti-apoptotic activities in a variety of cells (Funakoshi and Nakamura, 2003; Maina and Klein, 1999). Although the function of HGF in the nervous system has not been fully elucidated, it has recently been shown that HGF plays a strong neuroprotective

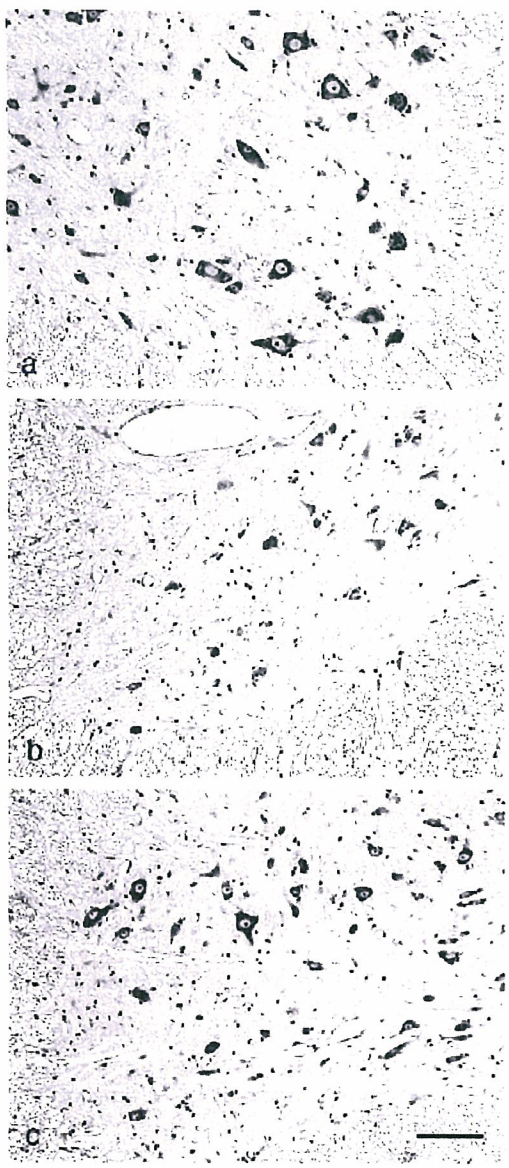

Fig. 6 – Photomicrographs of C7 spinal motoneurons at the contralateral (a) and ipsilateral (b, c) side 4 weeks after the right C7 spinal nerve avulsion and the treatment of AxCALacZ (b) or AxCAhHGF (c). Pictures (a) and (c) were taken from the same section. Nissl stain. Scale bar=100 μm.

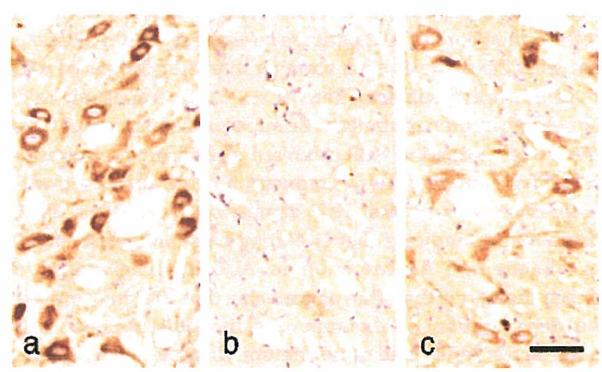

Fig. 7 – Photomicrographs of ChAT immunohistochemistry (a–c) of facial motoneurons at the contralateral (a) and ipsilateral (b, c) side 7 days after the facial nerve avulsion and the treatment of AxCALacZ (b) or AxCAhHGF (c). Pictures (a) and (c) were taken from the same section. Scale bar=50 μm.